High-Velocity Erosion of Sand

Heijmeijer, Oliver A.; Nobel, Arno J.; Keetels, Geert; Van Rhee, Cees

DOI
10.1061/(ASCE)HY.1943-7900.0001949

Publication date
2022

Document Version
Final published version

Published in
Journal of Hydraulic Engineering

High-Velocity Erosion of Sand

Oliver A. Heijmeijer[1]; Arno J. Nobel, Ph.D.[2]; Geert Keetels, Ph.D.[3]; and Cees van Rhee, Ph.D.[4]

Abstract: Dredging is the relocation of soil. Before the soil can be transported, it has to be loosened. This can be done hydraulically (jetting) or mechanically (cutting). Often, water jets are used to erode the soil layer. Over time, pickup functions have been derived to predict the amount of erosion corresponding to the flow conditions. However, existing pickup functions are inaccurate at high flow velocities. During the current study, erosion experiments have been done at high flow velocities (up to 4.7 m/s) corresponding to a bed shear stress of up to 60 Pa and a Shields parameter (θ) of up to 30. The results of these experiments were compared with a number of well-known data sets and pickup functions. **DOI: 10.1061/(ASCE)HY.1943-7900.0001949.**

Introduction

Erosion is governed by entrainment (the amount of sand that is picked up by the flow) and deposition (the amount of sand that settles down). When the pickup and deposition fluxes are not in equilibrium, the bed level changes. The velocity at which the level of the bed migrates is called the bed erosion velocity (v_e). The expression for the bed erosion velocity is

$$v_e = \frac{E_p - S}{\rho_s(1 - n_0 - c_{nb})} \tag{1}$$

where E_p = entrainment or pickup flux (kg/m^2/s); S = settling or deposition flux (kg/m^2/s); ρ_s = specific density of the grains (kg/m^3); n_0 = in situ porosity of the bed; and c_{nb} = near-bed volumetric concentration. The commonly used pickup function of Van Rijn (1984) matches most available data quite well in the low-velocity region (Shields parameter) $\theta < 1$; however, it largely overestimates available data at higher flow velocities ($\theta > 1$). It seems that no experimental data produced in a similar setup as Van Rijn (1984) at these higher flow velocities are available. To validate the pickup functions at high flow velocities and to gain a better understanding of the erosion process, new erosion tests at high flow velocities have been performed in the current study (further referred to as Boka). Comparing the results of this study to other erosion data at high flow velocities (Bisschop 2018) has raised new questions.

[1]Junior Production Engineer, Boskalis, Dredging Dept., Rosmolenweg 20, 3356 LK, Papendrecht, Netherlands (corresponding author). Email: oliver.heijmeijer@boskalis.com

[2]Senior Research Engineer, Boskalis, Corporate R&D, 3356 LK, Papendrecht, Netherlands. ORCID: https://orcid.org/0000-0001-8242-9350. Email: arno.nobel@boskalis.com

[3]Assistant Professor, Dredging Dept. of Engineering, Delft Univ. of Technology, Mekelweg 2, 2628 CD Delft, Netherlands. Email: g.h.keetels@tudelft.nl

[4]Full Professor, Dredging Dept. of Engineering, Delft Univ. of Technology, Mekelweg 2, 2628 CD Delft, Netherlands. Email: c.vanrhee@tudelft.nl

Note. This manuscript was submitted on June 2, 2020; approved on August 3, 2021; published online on February 26, 2022. Discussion period open until July 26, 2022; separate discussions must be submitted for individual papers. This paper is part of the ***Journal of Hydraulic Engineering***, © ASCE, ISSN 0733-9429.

Pickup Flux

Over the years, many studies have been done to figure out the complicated process of erosion. In this section, the models that were significant to this study are explained. All models are a combination of several principle terms and take the form of

$$\Phi_p = \frac{E_p}{\rho_s\sqrt{\Delta g d_{50}}} = n \cdot T^m \tag{2}$$

where Φ_p = dimensionless pickup flux; Δ = relative grain density, defined as $(\rho_s - \rho_w)/\rho_w$; g = gravitational acceleration constant (m/s^2); d_{50} = mean particle diameter (m); T = transport parameter; and n and m = empirical constants. The different pickup functions are as follows:

The pickup function of Fernandez Luque (1974) is

$$\Phi_p = 0.02 \cdot (\theta - \theta_{cr})^{1.5} \tag{3}$$

The pickup function of van Rijn (1984) is

$$\Phi_p = 0.00033 \cdot D_*^{0.3} \cdot \left(\frac{\theta - \theta_{cr}}{\theta_{cr}}\right)^{1.5} \tag{4}$$

The pickup function of Winterwerp et al. (1992) is

$$\Phi_p = 0.012 \cdot D_*^{0.3} \cdot (\theta^{0.5} - 1.3)^1 \tag{5}$$

The pickup function of Van Rhee (2010) is

$$\Phi_p = 0.000033 \cdot D_*^{0.3} \cdot \left(\frac{\theta - \theta'_{cr}}{\theta'_{cr}}\right)^{1.5} \tag{6}$$

The pickup function of Van Rhee and Talmon (2010) is

$$\Phi_p = 0.0025 \cdot (D_* - 2.4)^{0.3} \cdot (\theta)^1 \tag{7}$$

The pickup function of Cheng (2016) is

$$\Phi_p = 0.0001 \cdot D_*^{2.5} \cdot \left(F_* \exp\left(-\frac{40}{F_*}\right)\right)^1 \tag{8}$$

Finally, that of Van Rijn (2018) is

$$\Phi_p = 0.00033 \cdot D_*^{0.3} \cdot \frac{1}{\theta} \cdot \left(\frac{\theta - \theta_{cr}}{\theta_{cr}}\right)^{1.5} \tag{9}$$

where θ_{cr} = critical Shields number for particle motion initiation; θ'_{cr} = adapted critical Shields number according to Eq. (11); D_* = dimensionless particle diameter, $D_* = d_{50}\sqrt[3]{\Delta g/\nu^2}$; and

Table 1. Parameters of experiments considered during the present study

References	Flow velocity (m/s)	Shields, θ	Particle size, d_{50} (μm)	Porosity, n_0	Near-bed concentration, c_{nb} (%)	Bed length (cm)	Flume type
Fernandez Luque (1974)	—	—	900–3,300[a]	—	—	500–700	Descending bed
Van Rijn (1984)	0.5–1	0.3–1	130–1,500	0.4	0	2–5	Soil lift
Winterwerp et. al. (1992)	—	0.6–8.2	134–225	—	0–45	1,500–900	Descending bed (under an angle)
Roberts et al. (1998)	—	0.1–3.2	5–1,350	0.4–0.6	0	15	Soil lift
Van Rhee and Talmon (2010)	—	0–22	125–185	—	0–30	630	Descending bed
Cheng (2016)	0.27–0.99	0.01–0.54	230–860	0.4–0.44	0	1.5	Descending bed
Bisschop (2018)	1.5–6	2.5–450	51–562	0.4–0.5	20	630	Descending bed
BOKA	1–4.7	2.9–32	125	0.43–0.47	0	20	Soil lift

[a]The density of the grains was also varied during these experiments.

F_* = densiometric Froude number, $F_* = u/\sqrt{\Delta g d_{50}}$ where $F_* \propto \sqrt{\theta}$ and u is the depth-averaged flow velocity.

The original function of Van Rijn (1984) was based on and fitted to measurement data in the lower θ range ($\theta < 1$). In the recent update (van Rijn et al. 2019), the function has been adjusted and validated to the data of Bisschop (2018), which were in the higher θ range ($\theta > 1$). The data of Bisschop were produced in quite a different setup from the original data to which the function of Van Rijn (1984) was fitted.

In Table 1, one can see an overview of the parameters of the erosion experiments carried out by the different studies. There are two main types of tests:

- Erosion measured over a descending bed: bed height descends during the test due to erosion.
- Erosion measured over a soil lift: erosion takes place, but the bed remains at the same height because the sand column is pushed up by a lift.

The main differences between both principles are as follows:

- Developed concentration profile versus underdeveloped concentration profile: at the descending-bed tests, the erosion is measured at a location (on a long bed) where the concentration profile is well developed. At the tests with a soil lift, this is not the case because the bed is short an the concentration profile is still underdeveloped.
- Shear stress measured over a mobile bed ($\tau_{b,m}$) versus over a fixed bed ($\tau_{b,f}$): at the descending-bed tests, the shear stress is measured over the eroding bed. At the tests with a soil lift, the shear stress is measured directly upstream of the eroding bed over a rough floor called the fixed bed.
- Short bed versus a long bed: the length of the eroding bed in the soil lift is too short to show processes like dune formation. The length of the eroding bed in a descending bed setup is much longer and might show such processes.

Dilatancy Reduced Erosion

Van Rhee (2010) found that the pickup function of Van Rijn (1984) largely overestimated the pickup at high flow velocities. Van Rhee (2010) proposed to include the effect of dilatancy by adding a correction factor to the critical Shields number. The hydraulic gradient caused by the inflow of water will resist the dilation of the layers of sand. Van Rhee (2010) stated that the porosity of the sand bed must change from the in situ porosity n_0 to the maximum porosity n_l before it can be eroded. Combining Darcy's law for a hydraulic gradient and the necessary increase in porosity gives the following equation for the hydraulic gradient:

$$i = -\frac{v_e}{k_l} \cdot \frac{n_l - n_0}{1 - n_l} \tag{10}$$

where k_l = permeability of the soil at the maximum porosity n_l. This equation is only valid in the top layer of the sand bed. Combining the traditional critical Shields number and Eq. (10), Van Rhee (2010) defined a corrected Shields parameter as follows:

$$\theta'_{cr} = \theta_{cr}\left(\frac{\sin(\phi - \beta)}{\sin\phi} + \frac{v_e}{k_l} \cdot \frac{n_l - n_0}{1 - n_l} \cdot \frac{B}{\Delta}\right) \tag{11}$$

where ϕ = internal friction angle of the sediment; and $B = 3/4$ for single grains and $B = 1/(1 - n_0) \approx 1.7$ for a continuum approximation of the gradient at the bed surface. The left term inside the brackets of Eq. (11) includes the stability of a bed under an angle, β. In the current study, only horizontal beds were considered ($\beta = 0$); therefore, the term becomes 1. Van Rhee (2010) gave a criterion for high-velocity erosion, i.e., the moment when Eq. (11) should be used: when the second term between the brackets [Eq. (11)] becomes of order unity. Because all the values in this term except v_e are characteristics of the soil and are constant, Van Rhee (2010) defined the criterion for high-velocity erosion as follows:

$$\frac{v_e}{k_l} > \frac{n_l - n_0}{1 - n_l} \cdot \frac{B}{\Delta} \tag{12}$$

In short, Van Rhee (2010) suggested incorporating the effect of soil dilatancy by a modified threshold condition for individual particles at the bed surface. A similar approach has been proposed to incorporate downward and upward seepage effects on the initiation of sediment transport (Dey and Zanke 2004; Lu et al. 2010; Liu and Chiew 2012). Van Damme (2021) argued that it is also possible that internal friction in the mobilized and dilating top layer of the sand bed could restrict the erosion velocity.

Hindered Erosion

During erosion, the pickup flux is influenced by the near-bed concentration (c_{nb}). Bisschop (2018) called this influence hindered erosion. If the near-bed concentration is high, there will be grain–grain interaction causing grains to be knocked back onto the bed.

Another effect was described by Van Rhee and Talmon (2010), which continued on the theory that pickup is determined by turbulent bursts. Due to continuity, for a volume of water and grains that is transported from the bed, an equal volume must also be transported back to the bed. In other words, there is a net reduction in pickup. Van Rhee and Talmon (2010) reasoned that the theoretical maximum concentration that is picked up is the concentration of the bed: $1 - n_0$. Conversely, the theoretical maximum concentration that is returned to the bed is the near-bed concentration c_{nb}. Following this reasoning, they proposed the following reduction factor for the pickup flux:

$$E_{ph} = E_p \cdot \left(\frac{1 - n_0 - c_{nb}}{1 - n_0} \right) \tag{13}$$

When c_{nb} is low, the factor approaches unity and the pickup will not be reduced. In the theoretical case where c_{nb} reaches the bed concentration, the pickup is zero.

Erosion Regimes

During erosion, different regimes are recognized: the saltation regime and the bed load (or sheet flow) regime (Van Rijn 1984). The saltation regime describes a relatively slow flow in which the grains are lifted off of the bed individually and transported a certain distance. Single grains are lifted off of the bed due to lift, drag, and shear along the bed. In this regime, it looks like the grains are jumping, hence the name saltation. In the sheet flow regime, a layer of grains rolls/slides over the sand bed at relatively high flow velocities. Gao (2008) gave a theoretical model describing the transition between the saltation regime and the sheet flow regime as the bed shear stress (τ) increases (Fig. 1). At higher values of the bed shear stress, one finds a combination of saltation, rolling, and sliding. Sheet flow starts occurring when the bed shear stress overcomes the shear strength of the sand bed, causing whole layers of sand to start sliding.

Experiments

The experimental setup was the same as used by Nobel and van Rhee (2017), which was inspired by the setup of Van Rijn (1984). Fig. 2 shows a schematic overview of the closed-flow system used during the experiments. The main components are as follows:

- Pump: the water flow was regulated by an electrically driven centrifugal pump. A maximum velocity of 4.7 m/s could be achieved.
- Flow meter: to measure the height-averaged flow velocity, a flow meter was used. The range of the meter was 12 m/s, and it had a maximum error of $\pm 0.5\%$ of the measured value.
- Sediment lift: the sediment was added to the water flow by a rectangular $(0.188 \times 0.188 \times 0.800$ m) vertical sediment lift. The vertical velocity of the sediment lift was regulated by an electrically driven piston and measured by a distance sensor. This sensor had a range of 3 m and a maximum error of $\pm 0.05\%$ of the measured value. To obtain the velocity, the difference in distance was divided by the elapsed time.
- Flow pipe of galvanized steel $(w \times h = 0.188 \times 0.138$ m): to establish a defined flow with a developed boundary layer, a false floor with glued particles over a length of 5 m was placed in the flow pipe upstream of the sediment lift (Fig. 2). Due to the false floor, the flow height was reduced to 0.123 m.
- Shear stress measuring device: directly upstream of the sediment lift, the shear force exerted by the water flow on the bed was measured using a 0.4×0.17-m plate attached to a load cell. Without the load cell, this plate has one degree of freedom in the direction of the flow. When the load cell is installed, this movement is constrained, and the force in the flow direction (exerted by the flow) will be measured. This force was multiplied by the surface of the plate to obtain the (fixed) bed shear stress. The range of the load cell was 20 kg, and it had an maximum error of $\pm 0.023\%$ of the measured value.
- Differential pressure sensors: the differential pressure was measured at different lengths along the pipe. This measurement was used to calculate the bed shear stress upstream of the sand bed and to monitor the development of the boundary layer. The locations where the pressure sensors were connected to the setup were called pressure ports. These locations of the ports are indicated in Fig. 2. The range of the differential pressure sensors was 1,000 kPa (10 bar), and it had an maximum error of $\pm 0.25\%$ of the measured value.
- Pitot tubes: the velocity profile of the flow was measured directly upstream of the sediment lift. One pitot tube was installed in the ceiling and one tube was installed in the left wall (when looking in the direction of the flow) of the setup. In these two directions, both the horizontal and the vertical velocity profile can be measured. Cable glands were used in the holes of the setup to ensure that it remained watertight. The differential pressure over the pitot tube was measured with the aforementioned sensors. Using Bernoulli's principle, it was found that the range of the pitot tubes was 45 m/s, and the maximum error was $\pm 0.25\%$ of the measured value.

The following parameters were recorded: water flow rate, vertical velocity of sediment lift, pressure difference in flow pipe, and the load on the shear stress measuring device. The erosion process was recorded by a high-speed camera, and velocity profiles were measured at different flow velocities.

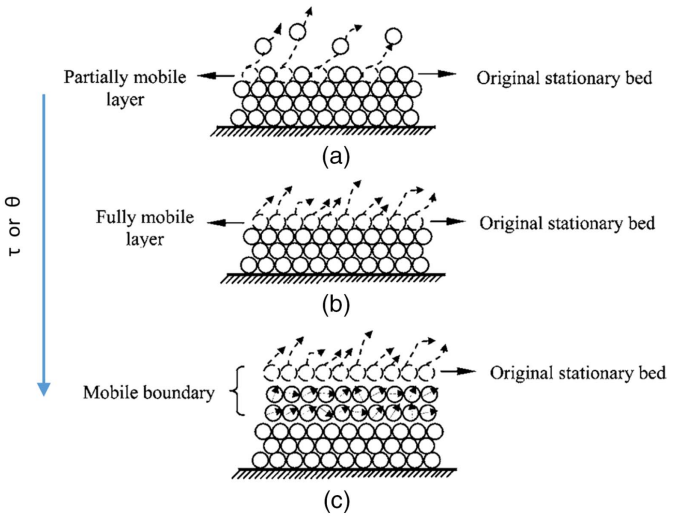

Fig. 1. Bed conditions: (a) saltation regime; (b) onset of sheet flow regime; and (c) sheet flow regime (Gao 2008).

Properties of Sand

During the experiments, Geba sand was used, which has a very narrow (uniform) grain-size distribution (Fig. 3) and d_{50} of 125 μm. Table 2 gives the main properties of the sand. Bisschop (2018) used the same sand for his experiments and measured the permeability of GEBA at different porosities (Fig. 4). These data points were used to determine the Kozeny-Carman constant (C_k) in the adapted Kozeny-Carman equation of Bear (1972)

$$k = C_k \cdot \frac{g}{\nu} \cdot d_{10}^2 \cdot \frac{n^3}{(1-n)^2} \tag{14}$$

The determined value of $C_k = 0.00387$. The calculated settling velocity of the GEBA sand is 0.12 mm/s, and the method of Ferguson and Church (2004) was used.

Measurement Procedure

A step-by-step description of how each measurement was performed is given in this section. The starting situation of this list

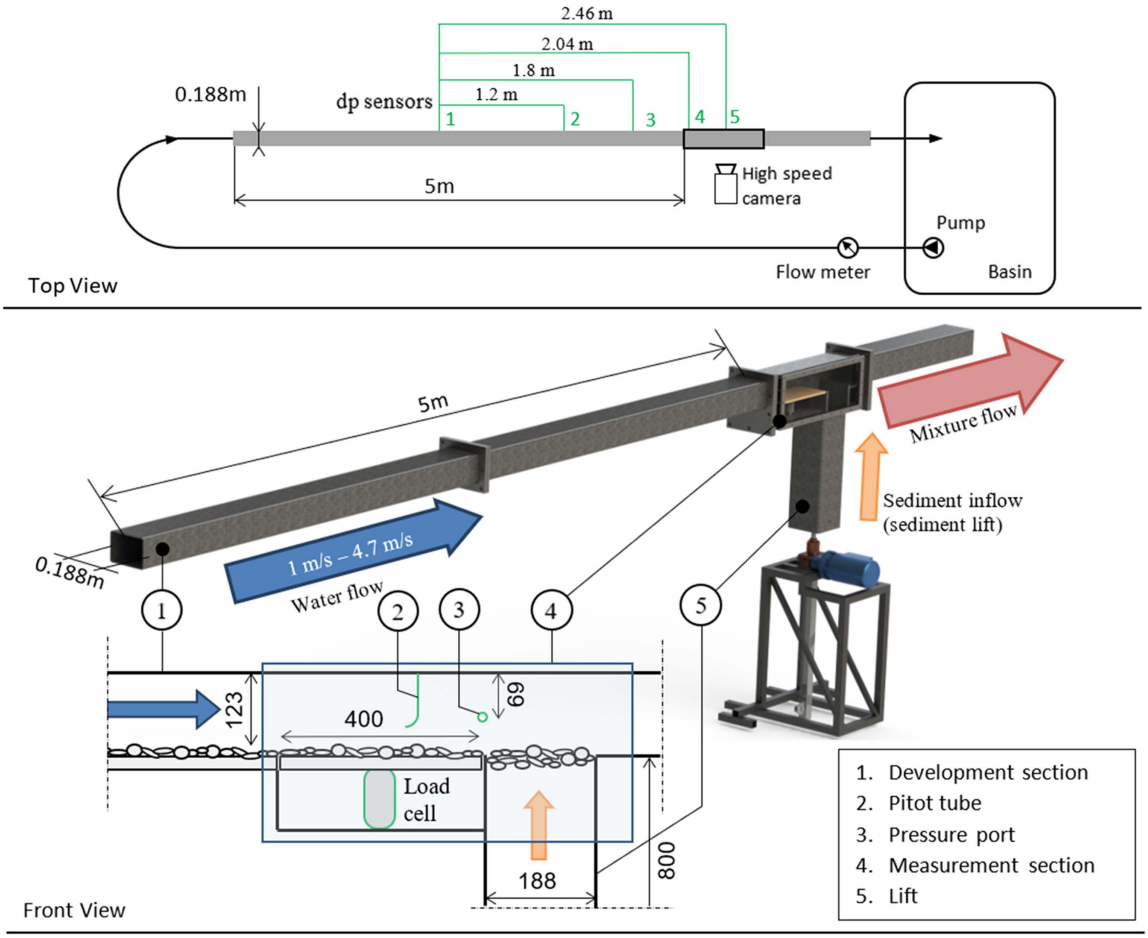

Fig. 2. Overview of setup. Dimensions in the measurement section are in millimeters. The depicted sand grains are magnified for clarity.

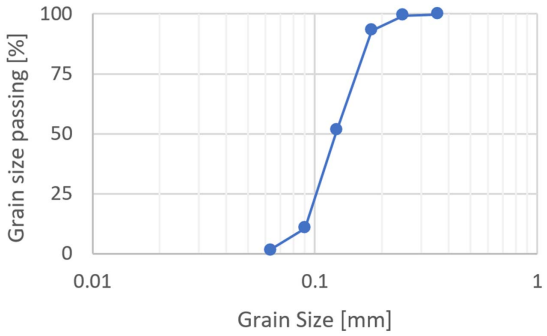

Fig. 3. GEBA grain-size distribution.

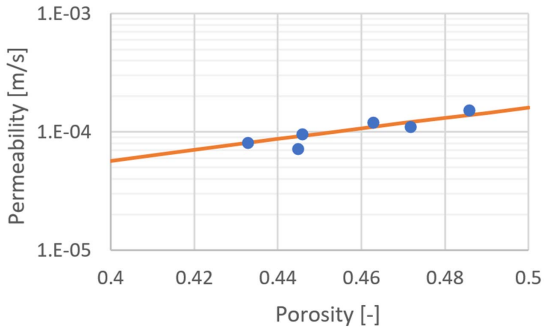

Fig. 4. Permeability (k) as a function of the porosity n_0.

Table 2. GEBA sand properties

Grain size				Porosity	
d_{10} (μm)	d_{50} (μm)	d_{60} (μm)	d_{90} (μm)	n_{max}	n_{min}
—	125	133	175	0.506	0.370

(Step 0) is as follows: setup empty (no water, no sand), window removed. The next steps are as follows:

1. Preset the sediment lift to different speeds. Estimate values faster, slower, and equal to the erosion velocity (depending on the flow velocity that will be tested). This can be done based on experience.
2. Fill the lift shaft with water.
3. Weigh the dry sand before slowly adding it to the water. Do this slowly to prevent entrainment of air and to ensure that the grains settle to a naturally occurring loose bed.
4. By means of vibration, increase the porosity of the sand bed to the desired value. The porosity is determined by using Eq. (15)

$$n_0 = 1 - \frac{m_s/\rho_s}{V_m} \tag{15}$$

where m_s = mass of the dry sand; and V_m = volume of the mixture.

J. Hydraul. Eng., 2022, 148(5): 04022005

5. Cover the sand bed with a piece of geotextile and pebbles to ensure that the bed stays intact while the rest of the setup is filled with water and the flow is brought up to the desired velocity.
6. Close the window and switch on the main pump to slowly fill the setup and bleed the air.
7. Start logging sensor signals, start recording camera footage, and bring the flow up to the desired velocity.
8. Run the lift. Experience showed that at the highest flow velocity, the bed needed approximately 5 s to become stable after starting the lift or changing the lift speed. It was chosen to only use the results of the tests where the bed was stable for a minimum of 10 s. At the highest flow velocity, one can test two lift speeds (total sand column depleted after 30 s). At lower flow velocities, it is possible to test three speeds (total sand column depleted after a maximum of 3 min).
9. When the lift has reached the top and the sand bed is completely eroded, stop the lift and retract it.
10. Bring the flow to a full stop, drain the setup, stop recording video, stop logging sensor signals, and remove the window. The setup is ready for the next sequence.

Erosion Velocity

For every flow velocity, at least three lift velocities were determined:
- lower limit (LL) (Fig. 5),
- erosion velocity (Fig. 6), and
- upper limit (UL) (Fig. 7).

The erosion velocity was said to be equal to the lift velocity when the eroding sand bed was horizontal and at equal height to the bed upstream. The judgement of the flatness of the sand bed was visually made with the aid of the footage of the high-speed camera. Stills from this footage are shown in Fig. 6, in which the sand bed (188 mm long) can be seen close up. Because the judgement of the flatness is subjective, an upper limit and a lower limit have been determined as well to indicate a bandwidth. When the lift speed was either too fast or too slow, one saw either a mound or a pit, respectively. It is also important to note that the experiments were only considered valid when the sand bed remained in a stable shape, i.e., equal erosion over the entire bed. The small pit on the left side of Fig. 6 (which initially occurred due to the transition from a fixed to a mobile bed), for instance, was not a concern because the size and shape remained the same throughout the measurement.

Shear Stress

As can be seen in the overview in the section "Pickup Flux," most of the pickup functions are proportional to the Shields parameter (normalized bed shear stress). It is the driving force of the erosion process. Therefore, the bed shear stress has been determined in three different ways during the experiments:
- direct measurement with the load cell,
- calculation of the bed shear stress based on the measured differential pressure, and
- calculation of the bed shear stress based on the measured velocity profile, using the logarithmic law.

Calculating the bed shear stress by means of the differential pressure required a special method because the walls of the pipe did not have the same roughness. As described previously, the bottom wall was coated with sand and therefore experienced a higher shear stress than the other, smoother, walls. Pugh and Wilson (1999) presented a method with which one can differentiate the different shear stresses of the different walls. The theory is based on the idea that the flow can be divided into two different sections: a bed-associated area A_b and a wall-associated area A_w (Fig. 8).

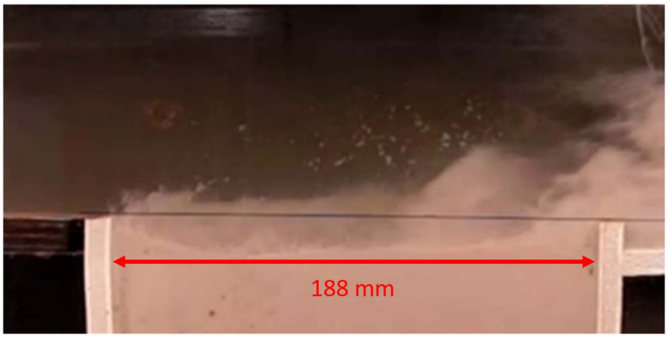

Fig. 5. Lower erosion velocity limit; lift speed too slow.

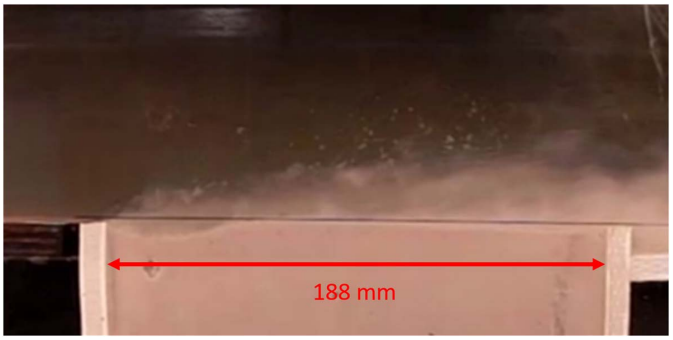

Fig. 6. Lift speed = v_e.

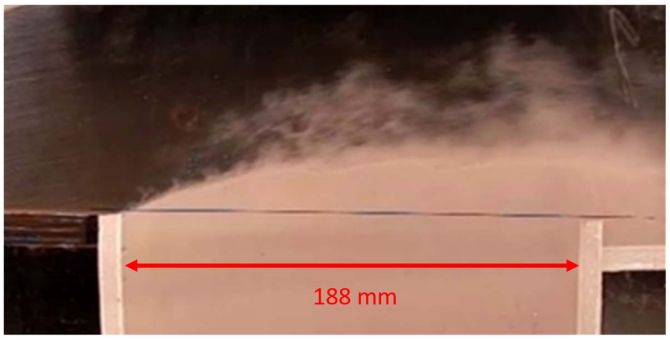

Fig. 7. Upper erosion velocity limit; lift speed too fast.

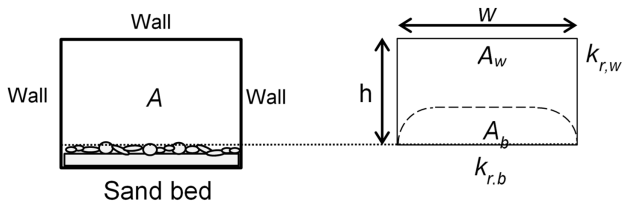

Fig. 8. Front view of pipe with bed and wall associated areas. The depicted sand grains are magnified for clarity.

The line that divides the two areas is the zero-shear line, and the pressure drop over a certain length must be the same in both areas

$$dp_b = \frac{\tau_b \cdot w \cdot l}{A_b} = dp_w = \frac{\tau_w \cdot (2h + w) \cdot l}{A_w} \tag{16}$$

where w and h = width and height of the pipe, respectively; l = length over which the pressure drop is measured; and A_b and A_w = bed- and

wall-associated areas, respectively. The corresponding shear stress can be calculated with the following equation:

$$\tau = \frac{\lambda}{8}\rho_w u^2 \tag{17}$$

where λ = Darcy-Weisbach friction factor. This friction factor can be estimated with the Colebrook (1939) equation

$$\frac{1}{\sqrt{\lambda}} = -2\log\left(\frac{k_r}{3.7D_h} + \frac{2.51}{\mathrm{Re}\sqrt{\lambda}}\right) \tag{18}$$

where k_r = corresponding roughness; and D_h = corresponding hydraulic diameter:

$$D_{h,w} = \frac{4A_w}{2h+w}; \qquad D_{h,b} = \frac{4A_b}{w} \tag{19}$$

Using the measured pressure drop and assuming values for the wall roughness $(k_{r,w})$ and the bed roughness $(k_{r,b} \approx 2 \cdot d_{90})$, the associated areas and the corresponding shear stresses can be determined by iteration.

Shear Stress over a Mobile Bed

There is a difference between the shear stress over a fixed bed (τ_f) and over a mobile (eroding) bed (τ_m). In a situation where the sand bed is fixed, the shear stress can be calculated as described previously. The friction over a mobile bed is not as straightforward. It is a quite complicated process that is not yet completely understood. There are factors that contribute to an imaginary roughness called effective roughness. Two common factors that contribute to this effective roughness are

- rolling and sliding grains, called a mobile layer (Gao 2008) (Fig. 1), and
- acceleration and deceleration of grains leading to a lag velocity (Greimann et al. 1999).

Pugh and Wilson (1999) stated that the effective roughness over a mobile bed is a function of the Shields parameter

$$\frac{k_{r,bm}}{d_{50}} = c \cdot \theta_b \tag{20}$$

This is an implicit function; iteration is needed to determine the roughness and shear stress. However, the function has more than one solution. For this reason, Bisschop (2018) derived his own function and fitted it to the data of his study

$$\lambda_b = 1.373 \cdot 10^{-9} \cdot Re_b^{1.247} \tag{21}$$

where λ_b = friction factor that can be used in Eq. (17); and Re_b = bed-associated Reynolds number, defined as $Re_b = u \cdot D_{h,b}/\nu$.

Test Data

In this section, the most important test results are discussed with the aid of graphs. In the Appendix, the main measurements are listed.

Bed Shear Stress

In Fig. 9, it can be seen that the three methods used for measuring the shear stress on the fixed bed (load cell, differential pressure, and velocity profile) match very well. There is a difference bandwidth of a maximum ±5%.

Erosion Regime

The ratio between the settling velocity and friction velocity is relatively small. This implies that particle transport is in the suspended regime based on the criterion $w_s/u_* < 0.6$ (Dey 2014), where w_s is the hindered settling velocity and u_* is the shear velocity. Existing calibrations of pickup functions of previous erosion studies (discussed in the overview in the section "Pickup Flux" and Table 1) also included data points in the contact-load and saltation regime.

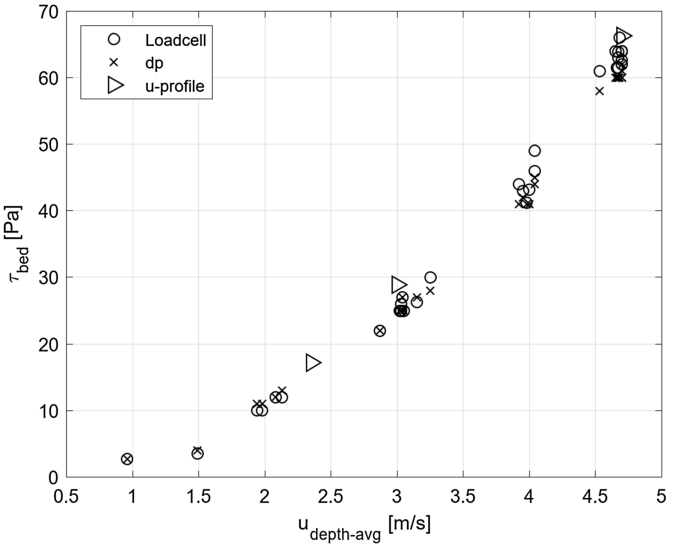

Fig. 9. Determined bed shear stresses as a function of the flow velocity.

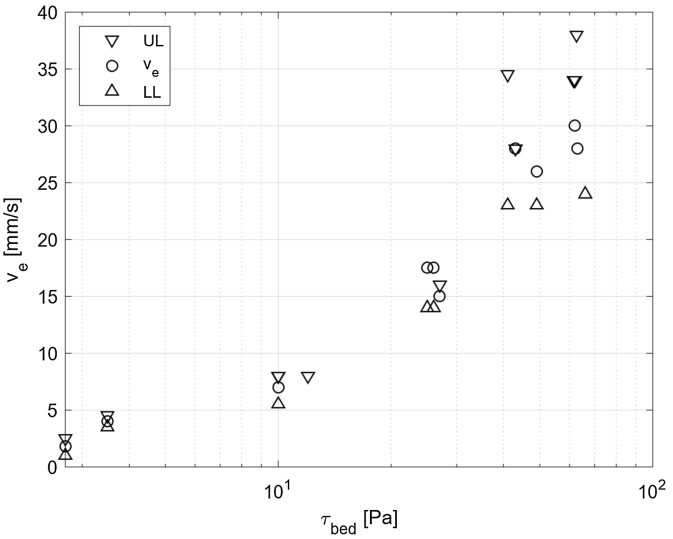

Fig. 10. Determined erosion velocity (and corresponding upper and lower limits) as a function of the measured bed shear stress.

Erosion Velocity Bandwidth

Fig. 10 shows the actual data points of v_e and the bandwidth as a function of the measured shear stress on the fixed bed directly upstream of the sand column. The demonstrated data points correspond to $n_0 = 0.43$. A summary of the data is listed in Table 3. The corresponding uncertainty bandwidth (error) is defined as follows:

$$ve_{\mathrm{error}} = \frac{\max(\mathrm{UL} - v_e, v_e - \mathrm{LL})}{v_e} \tag{22}$$

Table 3. Summary of measurement results

$u_{\text{depth-avg}}$ (m/s)	τ_f (Pa)	v_e (mm/s)	Bandwidth (mm/s)	ve_{error} (%)
1.5	3.5	4	3.5–4.5	±13
2	10	7	5.5–8.5	±21
4	43	28	22–34	±21
4.7	62	29	24–36	±24

Porosity

Roberts et al. (1998) showed that the porosity influences the erosion velocity. For the correction of the Shields parameter, Van Rhee (2010) validated the influence of porosity on the data of Roberts et al. (1998). The corrected pickup function [Eq. (6)] matched better with the data of Roberts et al. (1998) than the original function [Eq. (4)]. Because this influence was shown in the previous studies, the measurements of the current study have been performed at different values of porosity. It was found that the minimum possible porosity was $n_0 = 0.42$. This is because the lift was not powerful enough to overcome the friction between the sand column and the lift-shaft at lower values of n. With a porosity of $n_0 = 0.43$, the experiment could still be done. The maximum practically achievable porosity turned out to be $n_0 = 0.47$. When using Eq. (6) for high τ_{bed}, one would expect a large difference in erosion velocity when varying the porosity: up to a factor 1.6 between n_0 of 0.43 and 0.47 with a τ_{bed} of 62 Pa. This difference would be large enough to be measured in the current setup. However, from the data (Fig. 11), it was hard to conclude if the porosity had any influence on the erosion velocity because all points lie within the bandwidth that was described in the previous section. Also, the measured difference between the erosion velocities at a τ_{bed} of 62 Pa is between a factor 1.1 and 1.2 instead of the expected 1.6. Bisschop (2018) tested a larger range of porosities and concludes that the effect of porosity is negligible at higher shear stress.

Determination of Near-Bed Concentration

Because the near-bed concentration could not be measured with the setup of the current study, it was estimated from the video footage.

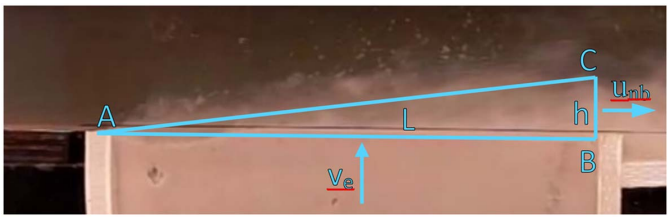

Fig. 12. Determination of near-bed concentration.

The sediment that is picked up from the bed will reach a certain height (h). The average concentration over that height is assumed to be the near-bed concentration. Fig. 12 shows the geometric relationship between the length L of the bed and the height h of the plume. It is assumed that, on average, no sediment passes through the line A-C. Therefore, the flux that passes through the line A-B will also pass through the line B-C. This relation is expressed as

$$\Phi_{AB} = v_e \cdot L \cdot (1 - n_0) = \Phi_{AC} = h \cdot u_{nb} \cdot c_{nb} \qquad (23)$$

where $(1 - n_0)$ = concentration of the bed; and u_{nb} = flow velocity near the bed.

The penetration length of the pitot tubes can be adjusted. This feature enabled the possibility to measure the velocity profile at a given height-averaged flow velocity. Using the velocity profiles, the average velocity over the height h was determined. When the height h was estimated from the camera footage, one could calculate the corresponding near-bed concentration.

Data Analysis

Fig. 13 shows the measured pickup rates of the current study and the other well-documented values in literature for $d_{50} = 125$ μm. It was observed that there is a large difference between the different functions. The measured pickup fluxes of Roberts et al. (1998) seemed to be lower than BOKA; however, the comparison was only with one data point of BOKA (Fig. 14).

A clear explanation for the mismatch cannot be given; however, there were some differences in the experiments that might explain the mismatch. Foremost, the height of the channel was 20 cm in

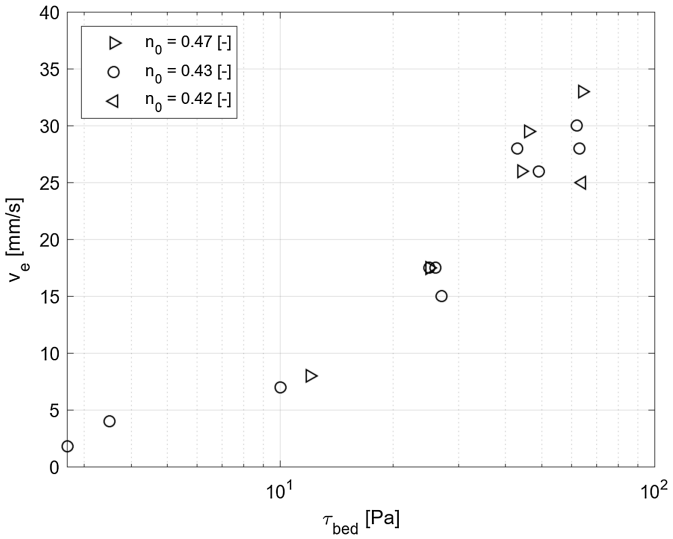

Fig. 11. Determined erosion velocity as a function of the measured bed shear stress for different porosities n_0.

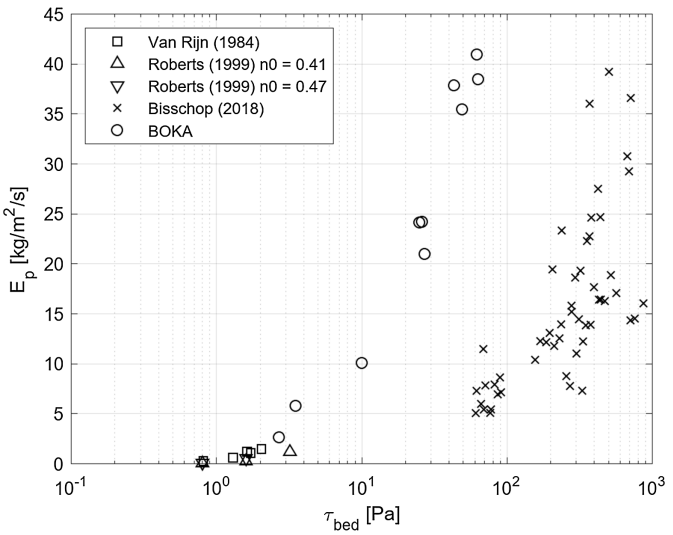

Fig. 13. Pickup rate E_p as a function of the bed shear stress (entire τ range).

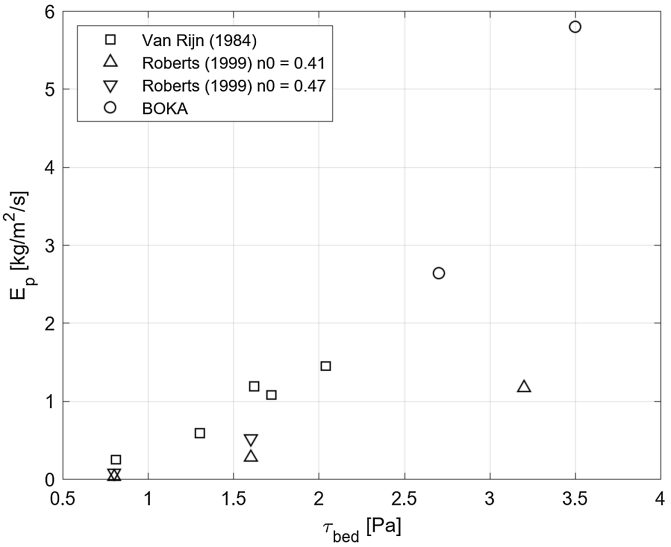

Fig. 14. Pickup rate E_p as a function of the bed shear stress (close up of low τ range).

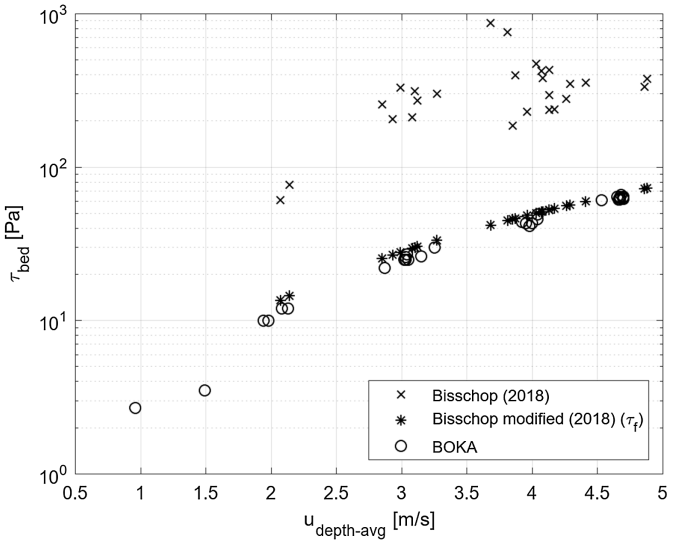

Fig. 15. Shear stress comparison between BOKA and Bisschop (2018).

both the studies of Van Rijn (1984) and the present study, but 2 cm in the the study of Roberts et al. (1998) (see also McNeil et al. 1996). This resulted in a reduction of the friction Reynolds number of a factor 10, which could affect the bed shear stress, drag, and lift force fluctuations and hence result in a lower particle pickup. Additionally, there could have been a difference in particle size because Roberts et al. (1998) used a Malvern particle sizer where the other studies did not. Lastly, other soil parameters that are unknown and decisive at low shear values, e.g., the particle shape (angularity/roundness), might be different.

The difference between the data of Bisschop (2018) and BOKA is significant, even though the range of flow velocities and the general dimensions of the setups are similar. The large bandwidth of the measured pickup rates at the same bed shear stress for the data of Bisschop (2018) is also remarkable. The main differences between both experiments are:

- location of the determined bed shear stress, and
- location of the measured pickup flux.

The effect of these differences on the data will be discussed subsequently.

Bed Shear Stress

The bed shear stresses of Bisschop (2018) were determined above the eroding (descending) sand bed, which is referred to as a mobile bed (τ_m with subscript m for mobile). The bed shear stress of BOKA was measured above a rough wall (similar roughness as the bed) directly upstream of the sand bed, which is referred to as a fixed bed (τ_f with subscript f for fixed).

Bisschop (2018) calculated the bed shear stress using the pressure difference over a length of 3 m over a mobile (and eroding) bed. The measured pressure difference, however, represented more processes (than only bed shear stress), which cannot be separated, i.e., rolling and sliding of the mobile bed (Gao 2008) and acceleration and deceleration of grains (Greimann et al. 1999).

As mentioned previously, the friction over a rolling bed is complicated and not fully understood. For this reason, the well-known bed friction on a fixed bed was measured in the current study similar to the other studies mentioned. It may not represent the actual shear stress experienced by grains that are being picked up, but it characterizes the strength of the flow in a dependable way.

To be able to compare apples with apples, each pickup value of Bisschop (2018) has been reassigned to a fixed bed shear stress using the method of (Pugh and Wilson 1999). Fig. 15 shows the calculated τ on a mobile bed (τ_m) and on a fixed bed (τ_f) as a function of the measured mean flow velocity. The measured shear stress of BOKA is also plotted in the figure for comparison. Because the velocity range and the general dimensions of the two setups are similar, it can be expected that the shear stresses on a fixed bed for both test series are almost the same.

Near-Bed Concentration

As described previously, the near-bed concentration has an influence on the pickup flux. Among others, the present study and the study of Bisschop (2018) had an inflow of clean water (no particles in the flow). Therefore, the near-bed concentration is zero just before the erodible sand bed. As sand is picked up during an experiment, the near-bed concentration increases in the direction of the flow until it becomes constant.

The pickup flux of Bisschop (2018) was measured in the middle of a long bed (6.25 m), where the near-bed concentration is relatively high ($c_{nb} \approx 0.2$). Therefore, the pickup of Bisschop (2018) can be referred to as hindered pickup. In the present study, the sand bed was only 0.188 m long. With this length, the near-bed concentration was still relatively low ($c_{nb} < 0.03$) and the effect of hindered erosion was negligible. Therefore, the pickup measured by BOKA was considered to be unhindered pickup.

The adjusted data of Bisschop (2018) was further converted from hindered to unhindered pickup by using the correction term of Van Rhee and Talmon (2010) [Eq. (7)]. The data is shown in Fig. 16, where it can be seen that the two studies are significantly closer together, but do not yet agree very well.

Comparison of Pickup Functions

Over the years, many pickup functions have been published, as discussed in the overview in the section "Pickup Flux." As mentioned previously, there are significant differences among these functions (Figs. 17 and 18).

From these plots, the following observations can be made:

- The pickup functions of Fernandez Luque (1974), Van Rijn (1984), and Roberts et al. (1998) overestimated the pickup

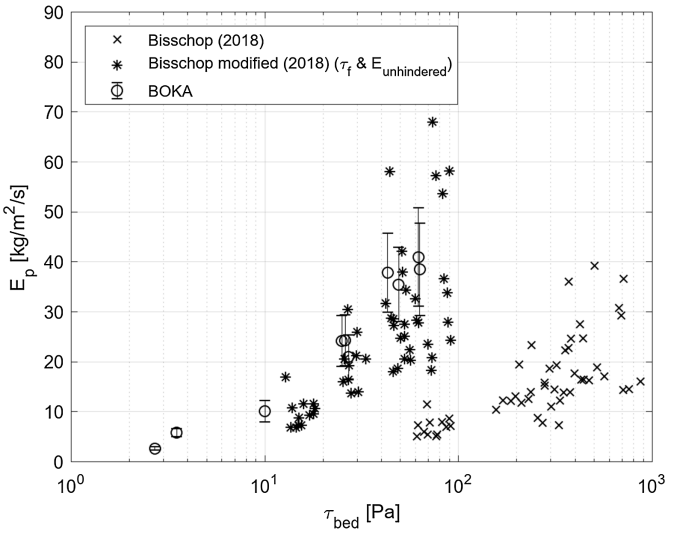

Fig. 16. Comparison of modified (τ_f and $E_{\text{unhindered}}$) pickup rates of Bisschop (2018) and present study.

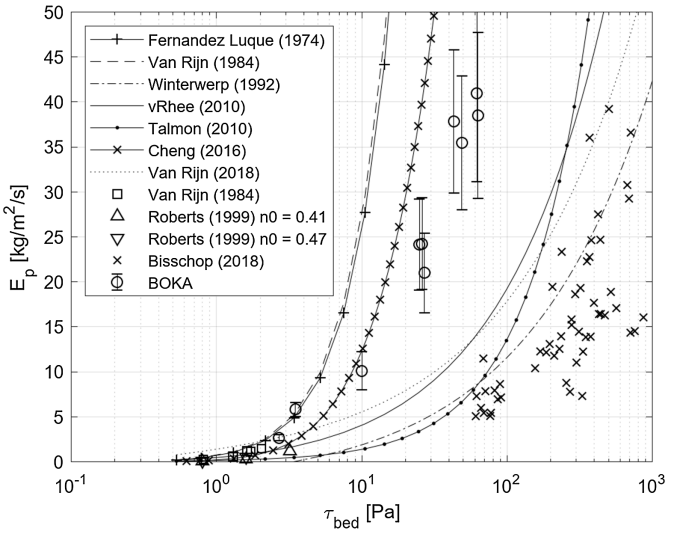

Fig. 17. Comparison of the different pickup functions.

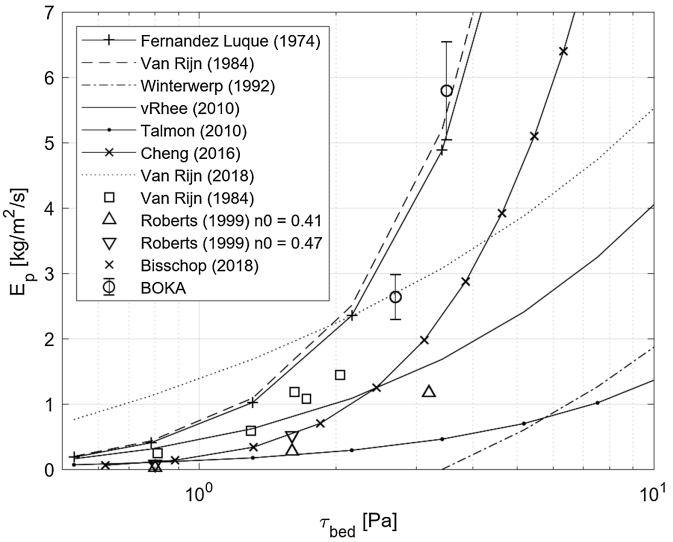

Fig. 18. Close-up of Fig. 17.

according to the data of the current study. This is surprising because the experiment method of the current study is similar to that of both Van Rijn (1984) and Roberts et al. (1998).

- The correction of Van Rhee (2010) and the pickup function of van Rijn et al. (2019) underestimated the pickup according to the data of the current study and overestimated the pickup according to the data of Bisschop (2018). Because the first two functions were validated with data produced in sediment-lift experiments, one would expect a better match with the data of BOKA rather than that of Bisschop (2018).
- The pickup functions of Van Rhee and Talmon (2010) and Winterwerp et al. (1992) seemed to have the best match with the data of Bisschop (2018). The first two have validated the pickup functions to the data of experiments with a descending bed (and τ_m), just like the latter. Therefore, it can be expected that the results are closer to the results of Bisschop (2018).
- The pickup function of Van Rijn (1984) did not match with the data of BOKA. The function was tuned to match the original data of Van Rijn (1984) ($\theta < 1$ and $\tau_b < 2$ Pa).

In the transport term T of Van Rijn (1984), the critical Shields number is in the denominator. This value is the minimum value necessary to initiate motion of the sediment and is difficult to determine precisely. Arguably, the parameter for initiation of motion should become less important as the shear stress (or Shields number) increases. However, when the critical Shields number is in the denominator, it will have influence over the entire range of θ.

In the function of Van Rhee (2010), the critical Shields value has been corrected to include the effect of dilatancy. The correction of Van Rhee (2010) was validated with data produced during the studies of Bisschop (1993) and Roberts et al. (1998) ($\tau_b < 6$ Pa). These experiments where also in the lower velocity range.

Bisschop (2018) noted that the effect of porosity of the prepared sand bed on the erosion velocity was negligible at high shield parameters ($\tau_b < 12$ Pa). The influence of dilatancy currently seemed to be too strong at higher Shields values in the function of Van Rhee (2010). Removing the critical Shields value from the denominator of the transport term T could solve the mentioned problems, although the critical Shields number, and thus the effect of dilatancy, still play a role when θ is in the order of magnitude of θ_{cr}.

Conclusion

In this study, experiments have been done using the same method and a similar setup as the study of Van Rijn (1984): a sediment lift, inflow of clean water, and the measurement of τ_b over a rough wall upstream of the eroding bed. The additions of the current study were the expansion of the range of flow velocity (and thus θ), and a more accurate way of measuring τ_b and v_e. Here, τ_b was measured with three independent methods (difference bandwidth of maximum $\pm 5\%$), and v_e was determined with the aid of a high-speed camera.

Using a comparable setup as Van Rijn (1984) and Cheng (2016) and an identical bed shear stress definition, it was observed that the scaling relations calibrated for $\theta < 1$ were inappropriate for $\theta \geq 1$. It was hypothesized that the observed differences could be explained by a change in the critical Shields parameter as a result of negative excess pore pressures that typically emerge in dilating soil layers under the act of shear. However, taking into account this effect by the theory of Van Rhee (2010), the formula of Van Rijn (1984) did

not give a satisfactory correspondence with the data. This suggests that the mechanism of solids pickup is fundamentally different at higher flow velocities (higher Shields parameter), and other factors than the erosion resistance need to be taken into account. The observed results also varied substantially with alternative erosion experimental setups and bed shear stress definitions. Therefore, ad hoc correction of pickup functions obtained from different setups and Shields parameter regimes is therefore discommended. The choice of a pickup relation should be made with care and depend on the context of the application.

It can be concluded that the variation in pickup functions was mainly attributable to the difference in validation data. The main differences are:

- the range in tested Shields value; the early pickup functions were only validated for a low Shields parameter,
- shear stress determined over a fixed or mobile bed differed significantly, and
- the near-bed concentration at measuring location; at large near-bed concentrations, the pickup function has to be corrected for hindered erosion.

Appendix. Data Acquired during Laboratory Tests

Test	Situ porosity, n_0	Flow velocity, u_{flow} (m/s)	Bed shear stress		Erosion velocity			Bed concentration, c_{nb}
			Load cell (Pa)	d_p (Pa)	LL (m/s)	v_e (m/s)	UL (m/s)	
47	0.42	4.7	64.0	62.0	—	—	28.0	0.05
48	0.42	4.7	64.0	60.0	—	25.0	—	0.05
49	0.42	4.7	63.9	60.0	23.0	—	—	0.05
50	0.43	1.0	2.7	2.7	1.0	1.8	2.5	0.02
31	0.43	1.5	3.5	4.0	3.5	4.0	4.5	0.02
26	0.43	2.1	1.2	13.0	—	—	8.0	0.03
27	0.43	1.9	10.0	11.0	5.5	—	8.0	0.03
28	0.43	2.0	10.0	11.0	—	7.0	8.0	0.03
15	0.43	3.0	25.0	25.0	14.0	17.5	—	0.05
16	0.43	3.2	26.3	27.0	14.0	17.5	—	0.05
19	0.43	3.1	—	26.0	—	—	21.0	0.04
22	0.43	3.0	27.0	27.0	—	15.0	16.0	0.04
17	0.43	4.0	43.2	41.0	—	28.0	—	0.06
18	0.43	4.0	41.2	41.0	23.0	—	—	0.06
24	0.43	4.0	43.0	42.0	—	—	28.0	0.06
25	0.43	4.0	49.0	45.0	23.0	26.0	—	0.06
38	0.43	4.7	62.6	60.0	—	—	38.0	0.05
39	0.43	4.7	62.0	60.0	—	30.0	34.0	0.05
40	0.43	4.7	61.5	60.0	—	—	34.0	0.05
41	0.43	4.7	63.0	60.0	—	28.0	—	0.05
42	0.43	4.7	66.0	60.0	24.0	—	—	0.05
36	0.47	2.1	12.0	12.0	—	8.0	—	0.03
32	0.47	2.9	22.0	22.0	16.5	—	—	0.05
33	0.47	3.1	25.0	25.0	—	17.5	18.0	0.05
37	0.47	3.3	30.0	28.0	—	—	22.5	0.05
34	0.47	4.0	46.0	44.0	—	29.5	32.0	0.06
35	0.47	3.9	44.0	41.0	22.5	26.0	—	0.06
43	0.47	4.7	61.5	60.0	—	—	36.0	0.06
44	0.47	4.7	64.0	61.0	—	33.0	—	0.06
45	0.47	4.5	61.0	58.0	27.0	—	—	0.06

Data Availability Statement

All data, models, and code generated or used during the study appear in the published article.

Acknowledgments

This study was commissioned by Boskalis, one of the largest dredging contractors in the world. All tests were executed in the hydrolaboratory of Boskalis in Papendrecht as part of the master's thesis of Heijmeijer (2019) at the Delft University of Technology.

Notation

The following symbols are used in this paper:

A = surface area (m^2);
A_b = bed-associated area (m^2);
A_w = wall-associated area (m^2);
C = empirical constant;
C_k = Kozeny Karman constant;
c_{nb} = near-bed volumetric concentration;
D^* = dimensionless particle size;
D_h = hydraulic diameter (m);

d_p = pressure difference (Pa);
$d_{10,60,90}$ = particle diameter at which 10%, 60%, and 90% of the sample mass is smaller (m);
d_{50} = median particle diameter (m);
E_p = pickup flux (kg/m^2/s);
F_* = densiometric Froude number;
g = gravitational acceleration (m/s^2);
h = height (m);
i = hydraulic gradient;
k = water permeability (m/s);
k_l = water permeability corresponding to n_l (m/s);
k_r = roughness height (m);
l = length (m);
m = empirical constant in pickup function;
n = empirical power constant;
n_l = porosity at which particles can be picked up;
$n_{\max}$ = maximum porosity;
$n_{\min}$ = minimum porosity;
n_0 = porosity of the bed;
Re = Reynolds number;
S = settling or deposition flux (kg/m^2/s);
T = transport factor;
u = flow velocity (m/s);
u_* = shear velocity (m/s);
u_l = vertical velocity of the sediment lift (m/s);
u_{nb} = flow velocity near the bed;
v_e = bed erosion velocity (m/s);
w = width (m);
w_s = hindered settling velocity (m/s);
β = bed slope angle (degrees);
Δ = relative density, $(\rho_s - \rho_w)/\rho_w$;
θ = Shields parameter;
θ_{cr} = critical Shields parameter;
λ = Darcy Weisbach friction coefficient;
ρ_s = specific density of the grains (kg/m^3);
ρ_w = water density (kg/m^3);
$\tau_{b,f}$ = bed shear stress over fixed bed (Pa);
$\tau_{b,m}$ = bed shear stress over mobile bed (Pa);
τ_w = wall shear stress (Pa);
ν = Kinematic viscosity of the fluid (m^2/s);
Φ_{AB} = flux through line AB;
Φ_{AC} = flux through line AC;
Φ_p = dimensionless pickup rate; and
ϕ = internal friction angle (degrees).

References

Bear, J. 1972. *Dynamics of fluids in porous media*. New York: Elsevier.

Bisschop, F. 1993. "Erosieproeven op zand met variatie in doorlatendheid." *Combinatie Speurwerk Baggertechniek* 510 (J714).

Bisschop, F. 2018. "Erosion of sand at high flow velocities." Ph.D. thesis, Dredging Engineering, Delft Univ. of Technology.

Cheng, N. 2016. "Comparison of sediment-pick-up rates over plane bed and dunes." *J. Hydraul. Eng.* 142 (12): 04016057. https://doi.org/10.1061/(ASCE)HY.1943-7900.0001204.

Colebrook, C. F. 1939. "Turbulent flow in pipes, with particular reference to the transition region between the smooth and rough pipe laws." *J. Inst. Civ. Eng.* 11 (4): 133–156. https://doi.org/10.1680/ijoti.1939.13150.

Dey, S. 2014. *Fluvial hydrodynamics*. Berlin: Springer.

Dey, S., and U. C. Zanke. 2004. "Sediment threshold with upward seepage." *J. Eng. Mech.* 130 (9): 1118–1123. https://doi.org/10.1061/(ASCE)0733-9399(2004)130:9(1118).

Ferguson, R., and M. Church. 2004. "A simple universal equation for grain settling velocity." *J. Sediment. Res.* 74 (6): 933–937. https://doi.org/10.1306/051204740933.

Fernandez Luque, R. 1974. "Erosion and transport of bed-load sediment." Ph.D. thesis, Dept. of Hydraulic Engineering, Delft Univ. of Technology.

Gao, P. 2008. "Transition between two bed-load transport regimes: Saltation and sheet flow." *J. Hydraul. Eng.* 134 (3): 340–349. https://doi.org/10.1061/(ASCE)0733-9429(2008)134:3(340).

Greimann, B. P., M. Muste, and F. M. Holly Jr. 1999. "Two-phase formulation of suspended sediment transport." *J. Hydraul. Res.* 37 (4): 479–500. https://doi.org/10.1080/00221686.1999.9628264.

Heijmeijer, O. A. 2019. "High velocity sand erosion." M.Sc. thesis, Dredging Engineering, Delft Univ. of Technology.

Liu, X., and Y. Chiew. 2012. "Effect of seepage on initiation of cohesionless sediment transport." *Acta Geophys.* 60 (6): 1778–1796. https://doi.org/10.2478/s11600-012-0043-7.

Lu, X., P. Cui, K. Hu, and X. Zhang. 2010. "Initiation and development of water film by seepage." *J. Mountain Sci.* 7 (4): 361–366. https://doi.org/10.1007/s11629-010-2052-9.

McNeil, J., C. Taylor, and W. Lick. 1996. "Measurements of erosion of undisturbed bottom sediments with depth." *J. Hydraul. Eng.* 122 (6): 316–324. https://doi.org/10.1061/(ASCE)0733-9429(1996)122:6(316).

Nobel, A. J., and C. van Rhee. 2017. "Erosion velocity of large grains subjected to a high uniform flow velocity." *J. Hydraul. Eng.* 143 (12): 04017054. https://doi.org/10.1061/(ASCE)HY.1943-7900.0001386.

Pugh, F. J., and K. C. Wilson. 1999. "Velocity and concentration distributions in sheet flow above plane beds." *J. Hydraul. Eng.* 125 (2): 117–125. https://doi.org/10.1061/(ASCE)0733-9429(1999)125:2(117).

Roberts, J., R. Jepsen, D. Gotthard, and W. Lick. 1998. "Effects of particle size and bulk density on erosion of quartz particles." *J. Hydraul. Eng.* 124 (12): 1261–1267. https://doi.org/10.1061/(ASCE)0733-9429(1998)124:12(1261).

Van Damme, M. 2021. "Detachment of dilatant soil due to high hydraulic shear stresses explained." *J. Hydraul. Res.* 59 (1): 51–60. https://doi.org/10.1080/00221686.2020.1714758.

Van Rhee, C. 2010. "Sediment entrainment at high flow velocity." *J. Hydraul. Eng.* 136 (9): 572–582. https://doi.org/10.1061/(ASCE)HY.1943-7900.0000214.

Van Rhee, C., and A. Talmon. 2010. "Sedimentation and erosion of sediment at high solids concentration." In *Proc., 18th Int. Conf. of Hydrotransport*. Rio de Janeiro, Brazil: Vereniging van Waterbouwers.

Van Rijn, L. C. 1984. "Sediment pick-up functions." *J. Hydraul. Eng.* 110 (10): 1494–1502. https://doi.org/10.1061/(ASCE)0733-9429(1984)110:10(1494).

Van Rijn, L. C., R. Bisschop, and C. V. Rhee. 2019. "Modified sediment pick-up function." *J. Hydraul. Eng.* 145 (1): 06018017. https://doi.org/10.1061/(ASCE)HY.1943-7900.0001549.

Winterwerp, J. C., W. T. Bakker, D. R. Mastbergen, and H. van Rossum. 1992. "Hyperconcentrated sand-water mixture flows over erodible bed." *J. Hydraul. Eng.* 118 (11): 1508–1525. https://doi.org/10.1061/(ASCE)0733-9429(1992)118:11(1508).